JOURNAL OF MATERIALS SCIENCE 11 (1976) 341–355

A comparative study of "gels" and oxide mixtures as starting materials for the nucleation and crystallization of silicate glasses

S. P. MUKHERJEE, J. ZARZYCKI
Laboratoire des Verres du C.N.R.S., Université de Montpellier 2, France

J. P. TRAVERSE
Laboratoire des Ultra-Réfractaires, C.N.R.S., Odeillo, France

Nucleation and crystallization behaviour of glasses in SiO_2–La_2O_3, SiO_2–La_2O_3–Al_2O_3 and SiO_2–La_2O_3–ZrO_2 systems were investigated using glasses prepared by the fusion of "gels" and the mixtures of oxides in solar/image furnace. Two methods for the preparation of multicomponent homogeneous non-crystalline products in the form of gels were developed. The phase separation, devitrification and micro-hardness of the above glasses were investigated in relation to the starting materials and the composition. The results show that the glasses made from gels are more homogeneous than those made from oxide mixtures. The phase separation characteristics of glasses made from gels are markedly different from those of glasses made from a mixture of oxides. The addition of Al_2O_3 to the binary SiO_2–La_2O_3 glasses improves the homogeneity but reduces the micro-hardness and the devitrification tendency, whereas the addition of ZrO_2 causes a considerable increase in micro-hardness and enhances the devitrification. The rates of nucleation and crystallization of glasses of different compositions made from gels are much higher than those made from the mixture of oxides. The formation of the high temperature crystal form, β–$La_2Si_2O_7$ is more evident with the crystallization of gel-glasses. When the rate of nucleation is low, (in the case of glasses from the mixture of oxides), the curve representing the relation between the micro-hardness and the time of heat-treatment shows a distinct minimum, whereas this minimum is not obtained with the gel-glasses. With most of the gel-glasses, the micro-hardness rises very sharply with the length of heat-treatment. The curve showing the relation between the micro-hardness and the volume fraction of the dispersed crystalline phase also gives a distinct minimum which can be explained on the basis of the fracture mechanism consisting of the processes of crack nucleation and of crack propagation around the dispersed crystalline particles.

1. Introduction

In recent years, the gel method of preparing starting compositions for phase equilibrium studies in silicate systems has been investigated by several workers [1–3]. It was also suggested [4] that this gelling technique could be a method for preparing homogeneous glass. More recently, another new method [5], similar to the gelling technique, but based on the polymerization reactions of alkoxysilane with other metal alkoxy compounds or suitable metal salts, has been reported for the preparation of glasses. However, no systematic investigations into the physico-chemical characteristics of the glasses prepared by the "gel" method have been published. The object of the present work is to investigate the suitability and advantages of using "gels" as the starting materials for the preparation of high temperature glasses and glass-ceramics. Hence, the following subjects were studied:

(a) the development of the methods of preparation of "gels" in SiO_2–La_2O_3, SiO_2–La_2O_3–Al_2O_3 and SiO_2–La_2O_3–ZrO_2 systems;

(b) the fusion of "gels" and oxide mixtures in solar or image furnace to produce glasses;

(c) the micro-structures and micro-hardness of the glasses thus prepared;

(d) the nucleation and crystallization characteristics of these glasses;

(e) finally; the micro-structures and micro-hardness of glass-ceramics produced from these glasses.

The glasses of compositions within the stable and metastable liquid–liquid immiscibility zone in the SiO_2–La_2O_3 system were investigated. The influence of small additions of a third component, Al_2O_3 or ZrO_2, on the phase separation, micro-hardness and volume crystallization characteristics was also studied.

2. Experimental

2.1. Preparation of gels

The compositions of glasses in the binary system is shown in Fig. 1 and Table I. The ternary compositions are based on binary compositions LS1 and LS2; they have been derived by the gradual replacement of SiO_2 by Al_2O_3 or ZrO_2.

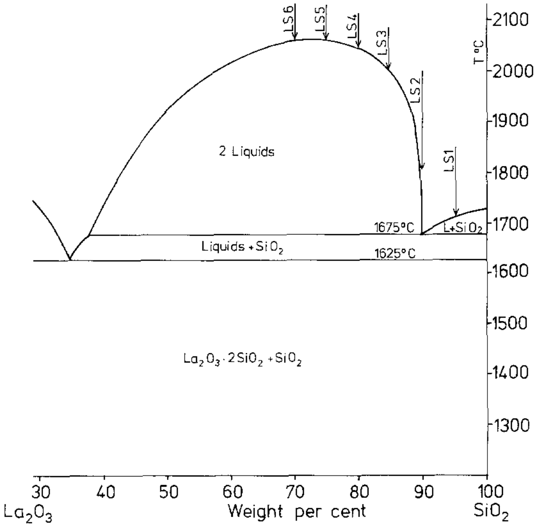

Figure 1 Phase diagram of SiO_2–La_2O_3 system showing the positions of the compositions investigated. After [37].

TABLE I

Glass no.	SiO_2		La_2O_3	
	wt %	mol %	wt %	mol %
LS1	95	99.04	5	0.96
LS2	90	97.99	10	2.01
LS3	85	96.85	15	3.15
LS4	80	95.60	20	4.40
LS5	75	94.21	25	5.79
LS6	70	92.68	30	7.32

The compositions of glasses in the SiO_2–La_2O_3–Al_2O_3 system and the SiO_2–La_2O_3–ZrO_2 system are given in Tables IIa, b and IIIa, b respectively. Since no chemical analysis of the glasses was made, the compositions indicated are the starting batch compositions before fusion.

Two methods for the preparation of gels were developed on the basis of the investigations of earlier workers [4, 5].

TABLE IIa Compositions in the SiO_2–La_2O_3–Al_2O_3 system based on binary composition LS1

Glass no.	SiO_2		La_2O_3		Al_2O_3	
	wt %	mol %	wt %	mol %	wt %	mol %
LAS1	94	98.42	5	0.96	1	0.62
LAS2	93	97.79	5	0.97	2	1.24
LAS3	92	97.16	5	0.97	3	1.87
LAS4	90	95.88	5	0.98	5	3.14

TABLE IIb Compositions in the SiO_2–La_2O_3–Al_2O_3 system based on binary composition LS2

Glass no.	SiO_2		La_2O_3		Al_2O_3	
	wt %	mol %	wt %	mol %	wt %	mol %
LAS5	85	94.66	10	2.06	5	3.28
LAS6	80	91.18	10	2.10	10	6.72

TABLE IIIa Compositions in the SiO_2–La_2O_3–ZrO_2 system based on binary composition LS1

Glass no.	SiO_2		La_2O_3		ZrO_2	
	wt %	mol %	wt %	mol %	wt %	mol %
LZS1	94	98.53	5	0.96	1	0.51
LZS2	93	98.00	5	0.97	2	1.03
LZS3	92	97.47	5	0.98	3	1.55
LZS4	90	96.40	5	0.99	5	2.61

TABLE IIIb Compositions in the SiO_2–La_2O_3–ZrO_2 system based on binary composition LS2

Glass no.	SiO_2		La_2O_3		ZrO_2	
	wt %	mol %	wt %	mol %	wt %	mol %
LZS5	85	95.20	10	2.07	5	2.73
LZS6	80	92.25	10	2.13	10	5.62

2.1.1. Method I

This method is based on the gelling of silica hydrosol Ludox AS (Du Pont Co, USA) containing other metal ions added in the form of aqueous solutions of lanthanum nitrate, aluminium nitrate and $ZrOCl_2 \cdot 8H_2O$. The gelling takes place primarily due to the change of pH. Details of the experimental methods for the preparation of gels in different systems are as follows.

(a) *SiO_2–La_2O_3 system.* La_2O_3 is weighed and dissolved in a minimum volume of dilute (1 : 1) HNO_3. The solution is evaporated to just dryness, and the residue is dissolved in distilled water to obtain a clear solution.

The pH of Ludox sol and of lanthanum nitrate solution are so adjusted before mixing that on mixing the pH of the final sol attains a value around 4.5. The sol is then left overnight for gel formation. A stiff, translucent gel is obtained.

(b) *SiO_2–La_2O_3–Al_2O_3 system.* The source of Al_2O_3 is $Al(NO_3)_3 \cdot 9H_2O$ (analytical grade, U.C.B. Belgium) which is dissolved in water. Then, lanthanum nitrate and aluminium nitrate solutions are added simultaneously to Ludox sol with constant stirring. The pH of the final sol is maintained around 3. A stiff translucent gel is obtained. The presence of Al^{3+} ions enhances the gelling process. This could be due to the fact that the formation of cross-linkages can be encouraged by the partial substitution of Al^{3+} for Si^{4+} [6].

(c) *SiO_2–La_2O_3–ZrO_2 system.* The procedure in this case is almost the same as in the case of the SiO_2–La_2O_3–Al_2O_3 system. An aqueous solution of $ZrOCl_2 \cdot 8H_2O$ (Fluka Co, Switzerland) is used as the source of ZrO_2; but, because of slight hydrolysis of this salt, a perfectly clear solution is not obtained. The pH of the final sol is adjusted to around 4.

2.1.2. Method II

This method is based on the polymerisation (i.e. hydrolysis and polycondensation) reactions of alkoxysilane with other metal alkoxides or with suitable metal salts in the presence of a limited amount of water to produce multicomponent inorganic gels probably with networks like $-\overset{|}{\underset{|}{Si}}-O-\overset{|}{\underset{|}{M}}-O-\overset{|}{\underset{|}{Si}}-$ where M is a metal atom, e.g. Al, Ti, etc.

It is reported [7] that the hydrolytic polycondensation products of alkoxysilane gives polyalkoxysilane networks composed of chains, rings or more complex combinations of silicon oxygen tetrahedra joined together by shared oxygen atoms reflecting in many ways the structure of silicates. The inclusion of a foreign element in the polyorganosiloxanes structure may be in a regular or random fashion, but this inclusion causes an increase in the polar character, and the stability of the Si–O–M linkages towards hydrolysis depend on the difference in electronegativity of silicon and metal atom [8].

The methods of the preparation of gels in the different systems are as follows.

(a) *SiO_2–La_2O_3 system.* The residue of lanthanum nitrate obtained by the evaporation of lanthanum nitrate solution is dissolved in ethyl alcohol. Tetraethoxysilane or tetramethoxysilane (technical grade, Fluka Co, Switzerland) is taken in a round bottom flask with a reflux condenser and an agitator. Ethyl alcohol of about $\frac{1}{2}$ volume of alkoxysilane is poured into the flask; the alcoholic solution of lanthanum nitrate is added to it with constant stirring. The solution is then heated to a temperature around 60° C with constant agitation and is kept under these conditions for 1 h. Then, a requisite amount of water is added dropwise.

The ratio of water (by weight) added and water required for complete hydrolysis of alkoxy compounds is in the range 0.7 and 0.9. The stirring and heating are continued for a period of 1 to 2 h after the addition of water. The solution is left overnight for gelation. A transparent stiff gel is formed.

(b) *SiO_2–La_2O_3–Al_2O_3 system.* The procedure is similar to that used for the binary system, but in this system, the source of Al_2O_3 is the aluminium isopropoxide or aluminium tert. butoxide (technical grade, Fluka Co, Switzerland). The fine powder of aluminium alkoxide in ethyl alcohol is added to the mixture of alkoxysilane and lanthanum nitrate in ethyl alcohol with constant stirring. The mixture is then heated to around 60° C with constant stirring and is kept under these conditions for 2 h to obtain a homogeneous solution. Then a requisite amount of water is added dropwise. The agitation and heating are continued for a further period of about 3 h, and the solution is then left overnight for gel formation.

(c) *SiO_2–La_2O_3–ZrO_2 system.* In this case, the source of ZrO_2 is the aqueous solution of $ZrOCl_2 \cdot 8H_2O$. Hence, alcoholic solutions of alkoxysilane and lanthanum nitrate are first mixed by agitating for about $\frac{1}{4}$ to $\frac{1}{2}$ h. Then $ZrOCl_2 \cdot 8H_2O$ in known volume of water is added with vigorous stirring. The temperature of the solution is then raised to 60° C with agitation. After $\frac{1}{2}$ h, a calculated amount of water (after taking into account the water added with $ZrOCl_2 \cdot 8H_2O$ solution) is added dropwise. The agitation and heating are continued for 2 h after the addition of water. The solution is then left for gelation.

2.2. Dehydration of gels

The dehydration of gels prepared by method I is done by stepwise heating in the following sequence; initial drying by an infra-red heater at 100 to 150° C; then the gel particles are ground to powder, dried at 500° C for 2 h, then at 900° C for 2 h, and finally at 1150° C for 2 h.

The dehydration procedure for the gels prepared by method II is almost the same as that stated above. But, as in this case, the gel particles become slightly brown during the initial drying at 100 to 150° C, at this stage, the particles are often moistened with a spray of water. After this initial drying, the particles are powdered and the powder is heated very slowly to 500° C in an open furnace and is kept at 500° C for 3 or 4 h for the removal of residual alkoxy groups until the powder becomes white. The steps following this are the same as in the case of gels prepared by method I.

2.3. Fusion of "gels" and mixtures of oxides in a solar or image furnace

2.3.1. Melting procedure

The products are prepared by fusion of the mixtures of oxides or the gels in air. Two types of furnace are used: a solar furnace and an image furnace with vertical axes. In both cases, the heating is done by concentrated radiation.

The powdered sample is placed on a cooled plate and is brought to the focal point of the apparatus [9]. The material is heated by the absorption of concentrated radiation. The radiation density is higher than 1500 $W\,cm^{-2}$. The radiation spectra are fairly similar in the solar furnace and in the image furnace [10]. The emitted energy is mostly in the visible range. Even solids which are either highly reflecting or quite transparent in this range of wave lengths could be melted and heated above the melting point.

The absorption of radiation in these cases could be enhanced by very fine grinding of the materials. However, in some cases with gels, it was necessary to add a small quantity of spectroscopically pure graphite to the gels to initiate fusion. But these specimens were not used for the systematic investigations reported in this article.

The quantity of material melted at a time is in the order of a gram. The melted specimens are in the form of spherules having diameters up to 10 mm. However, the uniformity of temperature is more easily obtained with smaller spherules having diameters 5 mm or less. This melting technique has the following advantages: a very high temperature above 2000° C can be easily obtained; the preferential evaporation of components is limited due to the short period of heating (about 30 sec.). The specimens are not contaminated by the substrate or support, and it is possible to devise simple means for splat-cooling. However, it should be noted that because of the difference in the absorption characteristics of the gels, the total time of treatment is slightly longer in the case of gels when compared with the time required for the mixture of oxides. The melting of the powder can be described as follows. At first, a very small liquid droplet is formed at a point in the powdered mass and, subsequently, this liquid droplet grows by the coalescence of finer droplets which appear in the vicinity of its periphery. In case of gels, the formation of finer droplets is less rapid and, as a consequence, the rate of growing of the initial droplet is lowered.

2.3.2. Cooling procedure

The sample after melting is rapidly moved away from the focal point of the furnace. The rate of cooling is in the order of 10^{2} ° C sec^{-1} during the initial period when the heat losses by radiation are preponderant. Samples of gels and of the mixtures of oxides were melted under the same technical conditions, but because of the difference in the absorption characteristics, the effective conditions of fusion are not strictly the same. However, the rate of cooling for specimens of similar size and composition in both cases should be nearly identical.

2.4. Characterization of products

Microstructures of glasses and glass-ceramics were investigated by electron microscopy using Pt-carbon replicas of mechanically polished and etched specimens.

The X-ray diffraction powder patterns of the specimens were obtained for the identification of the crystalline phases and also for the qualitative assessment of crystallinity. The patterns were taken either with a 114.6 mm Debye-Scherrer camera or with X-ray (Philips) diffractometer using Cu$K\alpha$ radiation with an Ni-filter.

Vicker's micro-hardness was determined using the micro-indenter attached to Reichert microscope "MeF". A load of 100 g was used. The standard deviations obtained with most of the non-crystalline specimens were in the range 10 to 15 kgf mm^{-2}.

3. Results and discussion

3.1. Crystallinity, micro-structure and micro-hardness of glasses before heat-treatment

In order to distinguish between the glasses of the same composition but made from different starting materials, the glasses prepared from oxide mixtures and those prepared from gels will be termed "ox-glasses" and "gel-glasses" respectively. The prefix "ox" or "gel" is used before the name of the composition; for example, ox-LS1 means glass LS1 made from oxide mixtures.

3.1.1. $SiO_2La_2O_3$ system

The compositions of glasses in this system are shown in Fig. 1 and Table I. The X-ray diffraction analysis shows that no devitrification occurs on cooling with the compositions LS1 and LS2. But volume crystallization occurs on cooling with compositions having 15% or more La_2O_3; and the extent of crystallization increases with increase of La_2O_3. The precipitating phase is β-$La_2Si_2O_7$, a high temperature form of lanthanum pyrosilicate. The composition containing 30% La_2O_3 is almost completely crystallized. No quantitative comparison between the crystallinity of the ox-glasses and gel-glasses has been made. But it is evident from the diffraction patterns that the crystallinity of ox-glasses is higher than that of gel-glasses, and the crystals precipitated with ox-glasses are larger.

The glass of composition LS1 is opalescent, but the transparency is higher with gel-glass. Glass LS2 is bluish-white in colour, and is almost opaque. The glasses of other compositions are completely opaque and bluish-white to white in colour.

The glass containing 5% La_2O_3 (LS1) shows phase separation in the form of spherical droplets rich in La^{3+} content dispersed in La^{3+}-poor silica matrix. It is evident from the micrographs, (Fig. 2a and b) that the micro-structure of phase-separated ox-glass differs from that of gel-glass in terms of uniformity and distribution of particle sizes. The micro-structure of ox-glass is not uniform throughout the specimen, large scale (0.3 to 0.6 μm) as well as fine scale (300 to 1000 Å) separation with a wide variation of particle size and shape occurs; whereas the micro-structure of gel-glass is more uniform and the size of the droplets is smaller and more uniform (600 to 1000 Å).

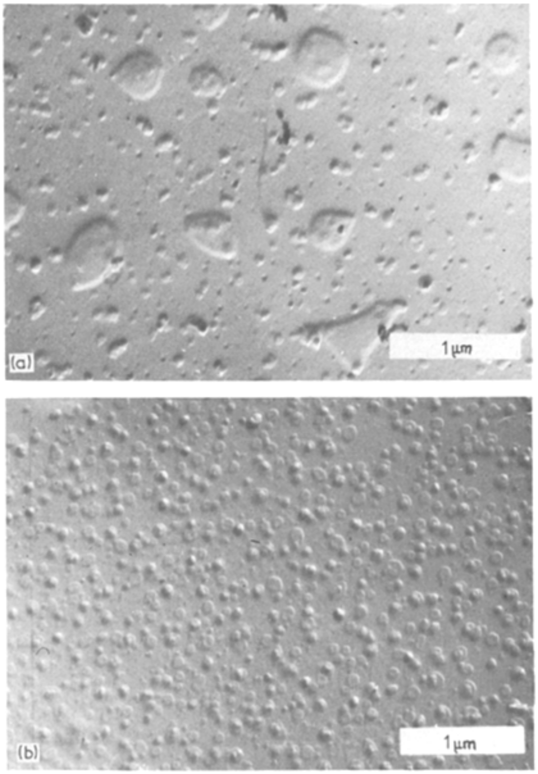

Figure 2 Electron micrographs of glass LS1 (5% La_2O_3) (a) from the mixture of oxides, (b) from the gel.

Fig. 1 indicates that the metastable liquid–liquid immiscibility zone at 1100° C obtained by extrapolation of the stable immiscibility curve (not shown in the figure) extends up to about 93% SiO_2.

On considering the lack of precision in extrapolation of such an asymmetric curve and also a slight preferential evaporation of SiO_2 during melting, it appears that the composition LS1 with 95% SiO_2 should fall within the metastable liquid–liquid immiscibility zone. The micro-structures obtained with subsequent compositions correspond to the micro-structures expected according to the phase diagram. With the composition LS2 (10% La_2O_3) also, the micro-structure of the ox-glass differs from that of gel-glass in the same manner as it does with the composition LS1, but because of extensive phase separation, the difference is not as distinct as in the case of composition LS1.

On further increase of La_2O_3, the phase separation is so extensive that it is not possible to distinguish between the micro-structures of ox-glasses and gel-glasses. The composition having 25% La_2O_3 (LS5) shows phase separation in the form of large-scale interconnecting phases. The precipitation of very fine (about 600 Å) crystals of β-$La_2Si_2O_7$ occurs in both phases, but the precipitation in terms of number density is less in the silica-rich phase.

The micro-structures obtained with gel-glasses can be explained on the basis of a more uniform distribution of La^{3+} ions in gels and, it seems, the homogeneity of compositions and the distribution of La^{3+} ions achieved during the gel formation is inherited to a great extent by the glass. However, the thermal history of preparation of glass (i.e. the time of melting and temperature of the melting) is the important factor to be considered. The presence of –OH groups which are not removed during the dehydration steps and are incorporated into the glass structure should enhance the kinetics of phase separation [11], but without having identical thermal histories and without quantitative measurement of volume fractions of dispersed phase in both cases, it is not possible to make any comments on the effect of OH^- groups during cooling.

The relation between the micro-hardness and glass-compositions in the SiO_2–La_2O_3 system is shown in Fig. 3. It is evident from the curve that the hardness of silica glass decreases with increasing La_2O_3 content up to 10% La_2O_3. However, on further addition of La_2O_3, the hardness increases due to the precipitation of fine crystals of lanthanum pyrosilicate in the silica matrix, and this increase which continues up to 25% La_2O_3 is primarily due to the increase in volume fractions of dispersed crystalline phases. Beyond this amount, the hardness appears to drop again; this could be due to several factors such as crystal size, percentage crystallinity, stresses, etc., which have not been investigated. It should be noted that the values of micro-hardness obtained with the ox-glasses and the gel-glasses do not differ significantly.

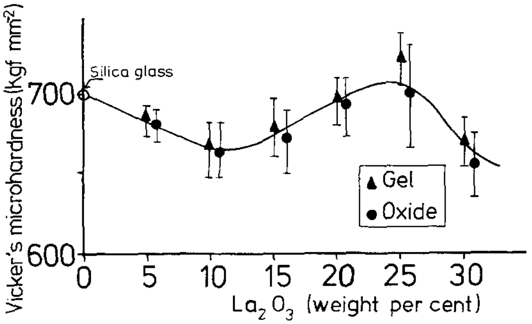

Figure 3 Relation between the Vicker's micro-hardness and composition of glasses in SiO_2–La_2O_3 system (the scatter = 2σ, where σ is standard deviation).

Although the mechanism of the formation of indentations in glass and the exact relation between the micro-hardness of glass and its mechanical properties are not yet well established, it may be stated that Vicker's micro-hardness values provide a measure of the yield stress of the glass-structure [12–15]. The reduction in hardness on addition of La_2O_3 to silica glass can be explained by assuming that La_2O_3 acts as a modifier in the glass structure.

It has been reported [12] that the addition of Na_2O or K_2O to silica glass causes a continuous decrease in Vicker's hardness. This continues up to a certain critical percentage of alkali and the decrease is more with K_2O. This decrease has been explained as the decrease of mean bond strength due to the breaking of Si–O–Si linkages. According to Weyl and Marboe [16], the high value of the micro-hardness of vitreous silica is the result of the combination of strong binding forces and the very low polarizability of the ions. The addition of alkali oxides increases the polarizability of all non-bridging oxygen ions, and so the hardness decreases. It is also reported [17] that the indentation hardness of different glasses can be correlated with their molar refractivities, the polarizability of the cations, and with softening temperatures of the glasses. The addition of lanthanum oxide to silica glass produces polarizable non-bridging oxygen ions due to the breaking of the Si–O–Si linkages. However, because of the large size of lanthanum ions (1.07 Å), its field strength (2.62) is not high enough to decrease the polarizability of non-bridging oxygen ions; therefore, the addition of La_2O_3 in small proportions to silica glass causes a reduction in hardness.

In order to obtain an idea of the estimated values of the Young's modulus, E, of the glass, a calculation has been made using the empirical equation of Makishima and Mackenzie [18]. The estimated values of E for glasses ox-LS1 and ox-LS2 are 668 and 658 kbar respectively. Hence, it seems that the Young's modulus of silica glass (730 kbar) decreases slightly on addition of La_2O_3. From the

E values, Vicker's micro-hardness H_v can be estimated using the following empirical equation developed by Yamane and Mackenzie [15],

$$H_v = C'(\alpha G \cdot K)^{1/2}$$

where C' is the proportionality constant to give the ratio of the stress to the resistance to deformation at the time when indentation ceases, α the ratio of average single bond strength to Si–O–bond strength, G and K the shear and bulk modulus, respectively

$$G = \frac{E}{2(1+\nu)}$$

$$K = \frac{E}{3(1-2\nu)}$$

Poisson's ratio, ν, can be estimated from the ionic volume fraction [15].

The constant C' as determined by these authors using measured values of H_v, K, and G for silica glass as 650, 3600 and 3200 kg mm^{-2} respectively, and by putting $\alpha = 1$, is 0.19. The value of H_v for silica glass obtained in the present experiment is 698 kg mm^{-2} which compares well with the values reported [12, 14]. Using this value of H_v, the constant $C' = 0.206$.

Using the above equation, the calculated micro-hardness values for ox-LS1 and ox-LS2 are 648 and 628 kg mm^{-2}, while the corresponding experimental values are 680 and 664 respectively. The estimated values are about 34 units lower than the experimental ones, but, on considering the several assumptions made for the deduction of the above equation, this discrepancy is possible.

3.1.2. SiO_2–La_2O_3–Al_2O_3 system

The compositions which have been investigated systematically are given in Table IIa. No crystallinity was detected with any composition. The transparency, as observed visually, increased with increase in Al_2O_3 content. The glasses of compositions LAS3, LAS4, appeared transparent. It was also observed that the transparency of gel-glasses was higher than that of corresponding ox-glasses.

On comparing the micro-structures of ox-glasses and gel-glasses, it was observed that the micro-structures of gel-glasses are more uniform and the size of the droplets is finer. In the case of ox-glasses, non-uniformity, in the form of large-scale separation and of wide variation in particle size exists, and this is more evident with the compositions LAS1 and LAS2.

As regards the influence of Al_2O_3 content on the phase separation, it may be stated that on addition of alumina the micro-structure becomes uniform, and the uniformity appears to improve until composition LAS3. It seems that a minimum amount of Al_2O_3 is needed to improve the uniformity. The sizes and volume fractions of the droplets were not estimated quantitatively, but the qualitative comparison indicates that the micro-structures obtained with the composition LAS2 show separation of the smallest droplets in high volume fractions.

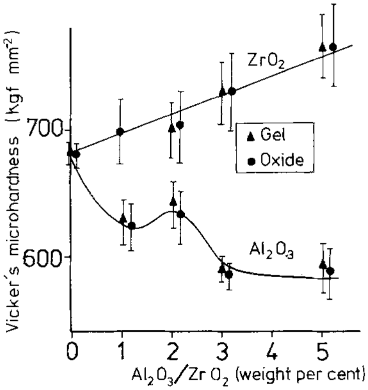

Figure 4 Influence on the micro-hardness of the addition of Al_2O_3 or ZrO_2 (by replacing SiO_2) to the binary composition LS1 (5% La_2O_3); (the scatter = 2σ).

The relation between the micro-hardness and the composition is shown in Fig. 4. It is evident that the hardness decreases on replacement of SiO_2 by Al_2O_3, but there is a slight anomaly with the composition LAS2 which will be discussed later.

A preliminary investigation of the compositions LAS5 and LAS6 based on binary composition LS2, has been carried out. No crystallinity was detected with these glasses. The nearly opaque binary LS2 glass changes to almost transparent glass on substitution of 5% of SiO_2 by Al_2O_3. The glass LAS6 appeared completely transparent. The influence of the addition of alumina in place of SiO_2 to the binary LS2 is similar to that as observed in the case of binary LS1. The micro-structures become more uniform, the size of the droplets becomes smaller.

The results on micro-hardness of compositions LAS5 and LAS6 show that a substitution of 5% of SiO_2 by Al_2O_3 causes a sharp fall (about 120 units) in the micro-hardness. But on further addition of Al_2O_3 no significant decrease is observed.

The higher uniformity of the micro-structures obtained with gel-glasses is probably due to the more uniform distribution of La^{3+} ions in gels as previously explained. The effect of the addition of alumina on micro-structures obtained by phase separation can be explained on assuming that Al^{3+} ions enter the network as AlO_4^- groups replacing Si^{4+} ions isomorphously. The positive charges required to maintain electroneutrality are supplied by La^{3+} ions which could fill in the holes near the tetrahedral sites occupied by AlO_4^- groups. Thus, the distribution of La^{3+} ions may be affected on small additions of Al_2O_3 to binary glass, and so, the nature of phase separation changes. This effect may be similar to the effect of small additions of Al_2O_3 to alkali silicate glasses [19].

The drop in micro-hardness on small additions of Al_2O_3 is due to the structural change caused by the introduction of Al^{3+} ions into the network as AlO_4 groups. If a cation goes into the interstices of the network, it will increase the overall bonding more than if it takes part in building or continuity of the structure, because, if its goes into the "holes" it is adding its own contribution to the strength in a smaller volume than if it goes into the structure building positions where it will increase the volume and, therefore, will make its own contribution to a larger volume of glass [12]. The lowering of Young's modulus on small additions of Al_2O_3 to a multicomponent base glass has been reported and explained by Lowenstein [20] as the entry of Al^{3+} ions into the network as AlO_4 groups. Moreover, since the field strength of the Al^{3+} ion is much less than that of the Si^{4+} ion, the isomorphous replacement will weaken the network at the point of substitution.

The slight increase in hardness with composition LAS2 (2% Al_2O_3) as compared to composition LAS1 (1% Al_2O_3) may be due to the smaller size of the spherical dispersed droplets obtained with LAS2. The increase of the ball indentation strength of phase-separated glasses with decrease in spherical particle diameter at constant volume fraction has been observed by Utsumi and Sakka [21].

3.1.3. SiO_2–La_2O_3–ZrO_2 system

The compositions that have been investigated systematically are given in Table IIIa. The glasses are bluish-white in colour and opalescent. The opacity increases with increase of ZrO_2, the composition LZS4 (5% ZrO_2) is opaque. No crystallinity is detected with compositions LZS1 and LZS2, but a slight volume crystallization occurs with compositions LZS3 and LZS4. The phases crystallizing are cubic or/and tetragonal ZrO_2 (ss) and α-$La_2Si_2O_7$, β-$La_2Si_2O_7$. The electron microscopic observation of glass ox-LZS1 shows that the addition of 1% ZrO_2 enhances the phase separation which is in the form of large interconnecting phases and is extremely non-uniform. No further investigation was made on this composition.

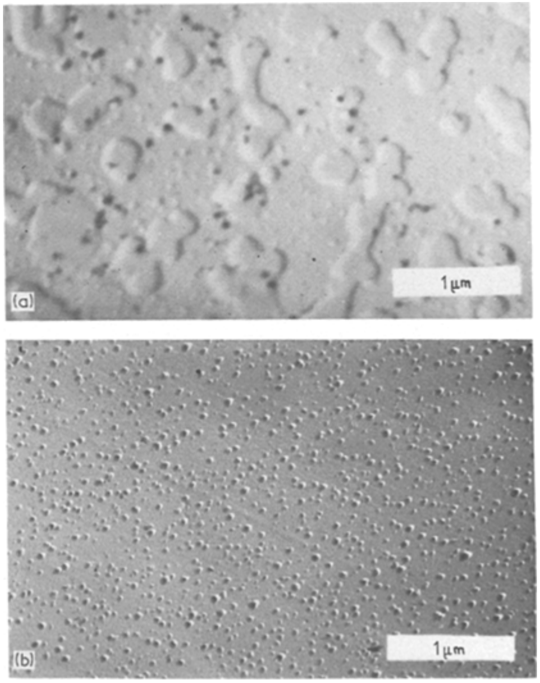

Figure 5 Electron micrographs of glass LZS2 (a) from the mixture of oxides, (b) from the gel.

The micro-structures of gel-glasses differ significantly in terms of uniformity of particle size and fineness. Electron micrographs of ox-LZS2 and gel-LZS2 are shown in Fig. 5a and b respectively. It should be noted that while in the case of ox-glasses, with increase of ZrO_2 content, the interconnectivity decreases, i.e. more discrete dispersed phases are obtained, in the case of gel-glasses, the morphology does not change appreciably.

The relation between the composition of glasses in the SiO_2–La_2O_3–ZrO_2 system and Vicker's micro-hardness is shown in Fig. 4.

The enhancement of phase separation on addition of ZrO_2, as is evident with ox-glasses, is due to the fact that as the Zr^{4+} ion, is not a network former, it takes up a position in the interstices, and because of its high field strength, enhances the phase separation. The development of significantly different micro-structure with gel-glasses may be attributed to the original gel-structure having Zr^{4+} ions distributed on a molecular scale. It has been suggested [22, 23] that the basic unit in a zirconia sol from $ZrOCl_2 \cdot 8H_2O$ is a cyclic tetramer $[Zr_4(OH)_8(H_2O)_8]^{8+}$ of about 10 Å diameter, and this could polymerize to form large polymeric groups. Hence, it may be anticipated that during the formation of gels, the basic units or smaller polymeric groups in a zirconia sol may co-polymerize with polymeric groups of a silica sol to give a uniform distribution of Zr^{4+} ions on a molecular level, and this structure may be inherited to a great extent by the glass structure.

The sharp rise in hardness of LS1 glass on addition of ZrO_2 is due to the fact that as the Zr^{4+} ions have a high field strength and are positioned in the interstices they increase the electrostatic bonding per unit volume and the increase in positive field strength is greater than the decrease in strength due to the breaking of Si–O–Si bond. Moreover, because of its high field strength, the Zr^{4+} ion decreases the polarizability of the non-bridging oxygen ions. It is reported [20] that the addition of ZrO_2, HfO_2, ThO_2 causes a considerable increase of Young's modulus of silicate glasses.

3.2. Crystallization characteristics of glasses and micro-structures and micro-hardness of glass-ceramics produced

3.2.1. SiO_2–La_2O_3 system

The volume crystallization was induced by one stage heat-treatment at 1150° C. The X-ray diffraction analysis shows that the rate of crystallization of gel-glasses is much higher than that of ox-glasses. The sequence of crystallization of different phases, the nature and amount of different phases obtained with both glasses are not the same, and change with their composition. This difference is most pronounced in the case of composition LS1. In the case of gel-LS1, the major phase precipitating during an initial period of ½ h, is β-$La_2Si_2O_7$, a high temperature form; the other phase is α-cristobalite. On further crystallization, α-$La_2Si_2O_7$ crystallizes, but the intensity of a strong line at 4.43 Å of this α-form obtained, does not match the intensity of the line at 4.48 Å in the pattern of the α-form reported [24, 25]; moreover, the intensity of this line increases with increase of the period of crystallization. It is most likely that this phase is a solid solution of α-$La_2Si_2O_7$ with SiO_2.

The crystallization of gel-LS1 is complete after 1 h heat-treatment. In the case of glas ox-LS1, the phase precipitating during the initial 2 h is α-$La_2Si_2O_7$; the pattern, in this case, matches well that of the α-form reported [25]. The crystallization of α-cristobalite is observed after 4 ½ h heat-treatment, and the crystallization is not complete even after 18 h heat-treatment.

The crystallization behaviour of glass LS2 is similar to that of glass LS1. The diffraction pattern of glass gel-LS2 crystallized for 2 h at 1150° C shows the presence of β-$La_2Si_2O_7$, α-$La_2Si_2O_7$ solid solution having a strong line at 4.49 Å, and α-cristobalite. The rate of crystallization of ox-LS2 is lower than that of gel-LS2. Unlike ox-LS1, in the case of ox-LS2, the crystallization of the high-temperature form, β-$La_2Si_2O_7$, is also observed.

Comparison of the crystallization behaviour of partially crystallized glasses, ox-LS5 and gel-LS5 shows that on heat-treatment at 1150° C for different period up to 9 h, the phases crystallizing with ox-glass are β-$La_2Si_2O_7$, α-$La_2Si_2O_7$, and the phases obtained with gel-glass are β-$La_2Si_2O_7$, α-$La_2Si_2O_7$ and α-cristobalite. Hence, the precipitation of α-cristobalite does not occur with ox-glass even on heat-treatment for 9 h at 1150° C. Unlike compositions LS1 and LS2, no strong line at 4.43 Å was obtained with gel-LS5.

The results of electron microscopic observation of glasses LS1 and LS2 are summarized in Table IV. The volume fractions, V_f, of the crystalline dispersed phase, the mean free distance λ, between

TABLE IV

Name of glass	Time of heat-treatment at 1150° C (h)	Volume fraction of dispersed crystalline phase (V_f)	Average diameter (d) of crystals (Å)	Mean distance (λ) between crystals (μm)	No. of nuclei per cm³ (n) × 10^{15}
Ox-LS1	½	0.046	405	0.840	1.322
	1	0.126	539	0.374	1.54
	2	0.156	550	0.298	1.79
Gel-LS1	¼	0.095	190	0.181	26.44
Ox-LS2	1	0.071	580	0.769	0.695
	2	0.154	722	0.397	0.787

the particles, and the average particle diameter, d, have been determined [26] from the electron micrographs of the specimens which do not show the crystallization of the matrix.

From the knowledge of V_f and d, an estimate of the number of crystals or number of nuclei per cm^3 has been made using the relation:

$$\text{number of nuclei per cm}^3, n = \frac{V_f}{\frac{4}{3}\pi\left(\frac{d}{2}\right)^3},$$

where d is average diameter of the crystal.

It is evident (Table IV) that the number of nuclei produced with gel-LS1, heat-treated for $\frac{1}{4}$ h under the present experimental conditions, is about 20 times higher than that obtained with ox-LS1 heat-treated for $\frac{1}{2}$ h. The micro-structures of ox-LS1 and gel-LS1 after $\frac{1}{2}$ h of heat-treatment are shown in Fig. 6a and b respectively.

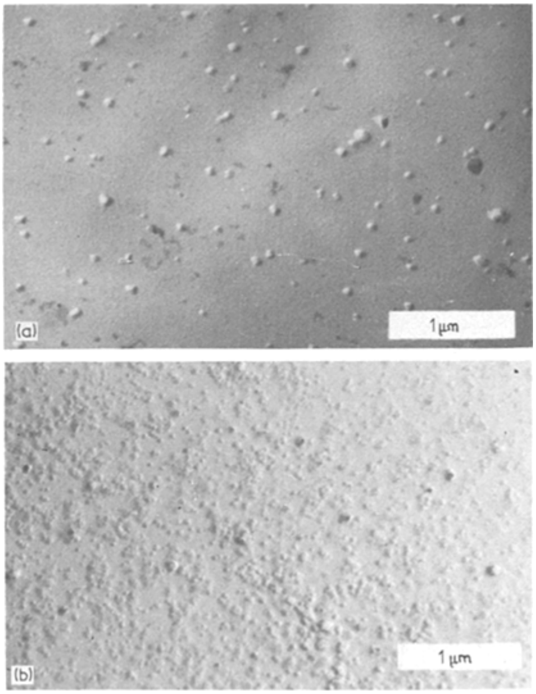

Figure 6 Electron micrographs of glass ox-LS1 and gel-LS1 after $\frac{1}{2}$ h heat-treatment at 1150° C (a) from the mixture of oxides, (b) from the gel.

However, it should be noted that although initially the micro-structure of as quenched gel-glass appears uniform, a non-uniformity in the form of larger droplets and separated "layers" develop in some parts during the initial period of heat-treatment. Subsequently, these separated phases crystallize to impart non-uniformity in the micro-structure of crystallized glass. It appears that coarsening, which has been enhanced due to the presence of –OH groups [11] and crystalization, occur simultaneously.

Comparison of the nucleation and crystallization rates of ox-LS1 and ox-LS2 (Table IV) shows that the increase of La_2O_3 content (ox-LS2) increases the rate of crystallization but decreases the rate of nucleation. The higher nucleation rate of ox-LS1 may be due to its phase-separation characteristics consisting of discrete droplets smaller in size than those obtained with ox-LS2.

The relation between the micro-hardness and the period of heat-treatment obtained with compositions LS1 and LS2 is shown in Figs. 7 and 8 respectively. It is evident that there is an extremely sharp increase in hardness in the case of gel-LS1, whereas in the case of ox-LS1, a slight decrease in hardness is observed during an initial period of $\frac{1}{2}$ h. The hardness then increases significantly during the next 4 h, but after this period, the increase is insignificant: hence a minimum is obtained in the curve. The shape of the curves obtained with composition LS2 (Fig. 8) is similar to that obtained with composition LS1, but the increase in hardness obtained with gel-LS2 is not as sharp as it is with gel-LS1.

The higher nucleation rates obtained with gel-glasses may be explained by assuming that –OH groups that have not been completely removed from the gels during the dehydration, are incorporated into the glass structure and subsequently act as nucleating agents as with fluoride ions in silicate glasses.

The nucleating action of fluoride ions has been explained by Mukherjee and Rogers [27] on the basis of the rearrangement of the double-chain ribbon-like anionic structure into single pyroxenoid chains due to the breaking of the linkage between SiO_4 tetrahedra on introduction of single charge fluoride ions into the network. The mineralizing action of –OH groups and fluorine is well known and is well explained by Buerger [28]. According to him, when an OH^- or F^- ion is substituted for an oxygen atom at the corner of a silicon tetrahedra, the substitution will remove a Si–O–Si link and transform the continuous silicate network into an aggregate of tiny silicate islands of molecular dimensions.

It has been reported by Verduch [29], in his work on the transformation of silicic acid to cristobalite, that at low temperatures, the presence of

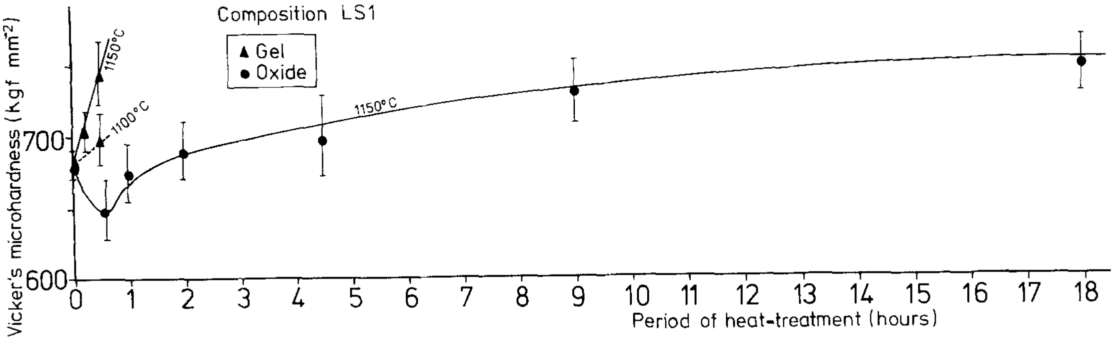

Figure 7 Relation between the Vicker's micro-hardness and the period of heat-treatment of glass LS1 (the scatter = 2σ).

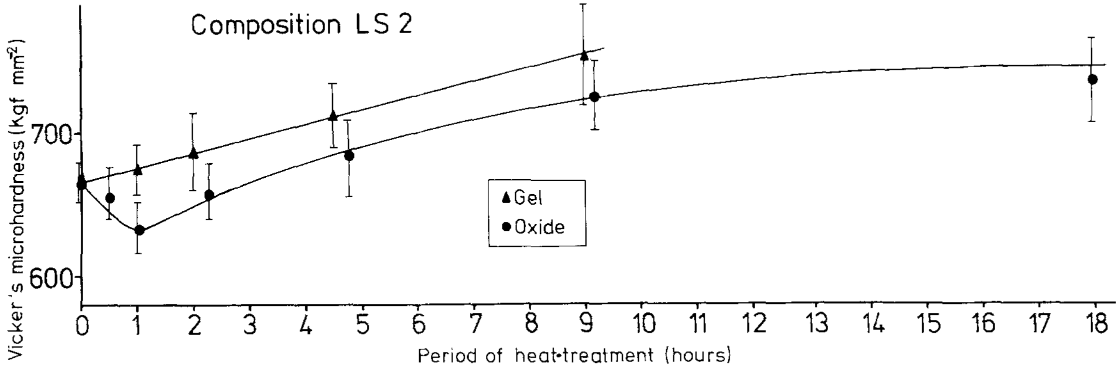

Figure 8 Relation between the Vicker's micro-hardness and the period of heat-treatment of glass LS2 (the scatter = 2σ).

water molecules has a much stronger depressing action on the nucleation potential barrier than it has on the growth barrier. It has been also shown [30] that the activation energies for viscous flow of silica glass decrease fairly smoothly as the number of either hydroxyl groups or chlorine atoms increase. The presence of 0.12 wt% hydroxyl groups reduces the activation energy from 170 kcal mol^{-1} to 122 kcal mol^{-1}.

The influence of hydroxyl groups in enhancing the crystallization rate of vitreous silica is well established by several authors [31, 32].

Hence, it may be concluded that the anionic structure as well as the distribution of cations in gel-glasses differs significantly from those of ox-glasses. This is also evident from the fact that the crystallization of the high temperature form, β-$La_2Si_2O_7$ is more pronounced with gel-glasses. The transition from β-$La_2Si_2O_7$ to α-$La_2Si_2O_7$ is a reconstructive type of transformation, according to Buerger's classification, and the temperature of transition is 1200° C [25]. In reconstructive transformation [33], on falling temperature, the units of the high temperature (open) structure may become relinked in an entirely different network. The relinking is not feasible with gel-glass because of the presence of –OH groups, so the structure remains open and, thus, the formation of the high temperature form should be facilitated.

To have a better understanding of the relation between the micro-hardness and the micro-structure of glass-ceramics, the volume fractions of dispersed crystalline phases were plotted against the micro-hardness and are shown in Fig. 9 for ox-LS1 and

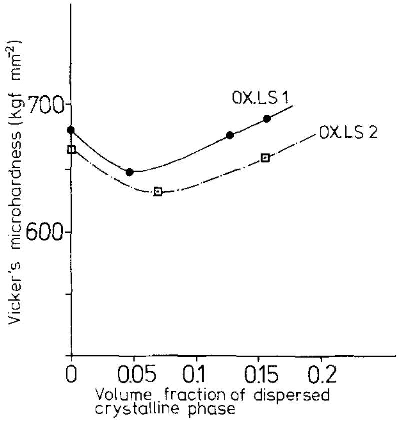

Figure 9 Relation between the Vicker's micro-hardness and the volume fraction of dispersed crystalline phase.

ox-LS2. The relation between the micro-hardness and volume fractions of crystalline phase of glass-ceramics as obtained in the present investigation can be adequately explained on considering the theories of the mechanical strength of glass-crystal composites, proposed by Hasselman and Fulrath [34] and Miyata and Jinno [35], and recently analysed, with special reference to glass-ceramics, by Zarzycki [36].

According to the theory of Miyata and Jinno [35], the fracture mechanism consists of two processes: (a) crack nucleation and (b) crack propagation around the dispersed phases. At lower volume fractions of dispersed phases, macroscopic fracture will occur as a result of the growth of micro-cracks originating through a nucleation process in the matrix close to the glass-crystal composites. In this case, strength decreases with the proportion of dispersed phase. At higher volume fraction, when interparticular distances are small, the micro-cracks formed by the nucleation process may cease to grow once they reach the mean distance between the dispersed phase, but after some increase in the applied tensile stress, these cracks may propagate around the dispersed particles by a process involving a high surface energy in the cracks. In this case, strength is an increasing function of the volume fraction. These two processes are represented by two curves which intersect in a certain volume fraction depending upon the grain size.

As a result, the measured strength–volume fraction curve will have a minimum near the point of intersection of the two curves, and the minimum will shift to lower volume fractions with smaller particle sizes and the strength reduction is less with finer particles. Hence, the minimum observed in the micro-hardness versus volume fraction curve is in agreement with the above theory, and a slight shift of the minimum obtained with ox-LS2 may be ascribed to its slightly larger particle size which is around 720 Å compared to 550 Å obtained with ox-LS1.

3.2.2. SiO_2–La_2O_3–Al_2O_3 system

In this system, the crystallization behaviour of two compositions LAS2, LAS4, based on binary LS1 were investigated. The volume crystallization was done by one stage heat-treatment at 1150° C for different periods. The results of X-ray diffraction studies show that as for the binary composition, the rate of crystallization of gel-glass is higher than that of ox-glass. However, the rate of crystallization of gel-glasses containing Al_2O_3 is considerably less than that of binary glass gel-LS1. The same result is obtained with ox-glasses. Hence, the addition of Al_2O_3 diminishes the overall rate of crystallization. However, surface crystallization in the form of a thin layer was observed with glasses containing Al_2O_3. It was also observed, particularly with ox-glasses, because of their lower rate of crystallization, that the rate of surface crystallization of α-cristobalite is higher with glasses containing Al_2O_3 compared to the binary ox-LS1.

The crystalline phases appearing are the same in both gel- and ox-glasses. One of them is α-cristobalite. The other is most likely an α-$La_2Si_2O_7$ solid solution as obtained with binary gel-LS1, but it needs more investigation for definite identification. The isomorphous replacement of Si^{4+} by Al^{3+} reduces the rate of crystallization of lanthanum silicate phase, but increases the rate of surface crystallization of α-cristobalite. The effect of the addition of Al_2O_3 on the crystallization rates of $La_2Si_2O_7$ and α-cristobalite can be explained if it is assumed that the effect of the replacement of Si^{4+} by Al^{3+} ions in lanthanum silicate glass is similar to the effect of addition of Al_2O_3 in alkalisilicate glass where the devitrification tendency is reduced on a small addition of Al_2O_3 [19].

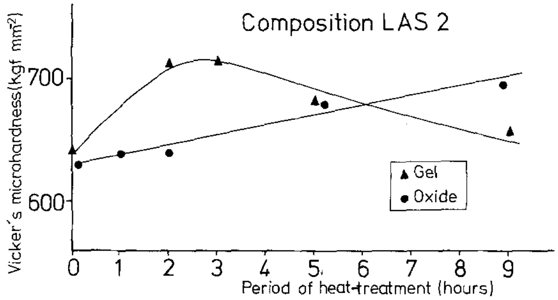

Figure 10 Relation between the Vicker's micro-hardness and the period of heat-treatment of glass LAS2.

The electron micrographs supported by the results of the X-ray powder diffraction patterns of the heat-treated glasses indicate that the droplets as well as the matrix crystallize slowly with increase in periods of heat-treatment, and the rate of crystallization is higher with gel-glasses. The relation between the micro-hardness and the period of heat-treatment of glass LAS2 is shown in Fig. 10.

The sharp increase in hardness with gel-glass is due to its higher crystallization rates of both droplets and the matrix. The decrease of hardness after reaching a maximum may be due to several factors developed due to the grain growth and crystallization of the matrix which have not been investigated.

3.2.3. SiO_2–La_2O_3–ZrO_2 system

In this system, the crystallization behaviour of three compositions LZS2, LZS3 and LZS4 were investigated. The volume crystallization was induced by one stage heat-treatment at 1150° C for different periods. The rate of crystallization of gel-glass is much higher than that of ox-glass.

In the case of ox-glass, during the initial period of heat-treatment, the precipitating phases are cubic and/or tetragonal ZrO_2 (ss) and α-$La_2Si_2O_7$. The period of heat-treatment necessary for the onset of crystallization of α-cristobalite increases with increase of ZrO_2 content. With ox-LZS2, the crystallization of α-cristobalite was detected after $4\frac{3}{4}$ h of heat-treatment; with ox-LZS3, α-cristobalite was not detected even after 18 h. In the case of ox-glasses, the silica matrix crystallizes less readily, when compared with gel-glasses. The phases precipitating with gel-glasses are the same as those obtained with ox-glasses. With gel-LZS2, the onset of crystallization of silica was observed after 1 h of heat-treatment. With gel-LZS3 and gel-LZS4, the crystallization of silica was observed after 2 h of heat-treatment.

The micro-structures of gel-glasses and ox-glasses developed after different periods of heat-treatment differ markedly in nature. In the case of ox-glass, the micro-structure after 2 h heat-treatment shows the coarsening of separated phases, resulting in a large-scale phase separation with particles of different shapes and sizes (0.2 to 0.5 µm). The precipitation of large (0.8 µm) cubic and/or tetragonal ZrO_2 (ss) crystals also occurs. The coarsening proceeds on further heat-treatment up to $4\frac{3}{4}$ h. The micro-structure obtained after 9 h heat-treatment shows distinct crystalline particles growing within the separated phases.

In the case of gel-glass, no coarsening and no precipitation of large ZrO_2 crystals occur. During an initial period of 1 h, the micro-structure shows the separation of fine droplets which might have very slight crystallinity; on further heat-treatment, the dispersed droplets crystallize without coarsening and so the sizes of the crystals which are around 800 Å are almost the same as the initial size of the droplets. The matrix starts to crystallize after 2 h heat-treatment. This difference in micro-structures and the crystallization behaviour of the gel-glasses could be attributed to the original gel-structure having Zr^{4+} ions distributed in a molecular scale as previously explained. The higher rate of crystallization of α-cristobalite in gel-glasses is due to the presence of hydroxyl groups incorporated in the glass-structure.

The relations between the micro-hardness and the period of heat-treatment obtained with compositions LZS2, LZS3 and LZS4 are shown in Fig. 11. This sharp fall in micro-hardness during the initial period of heat-treatment obtained in the case of ox-glasses is most likely due to the following factors:

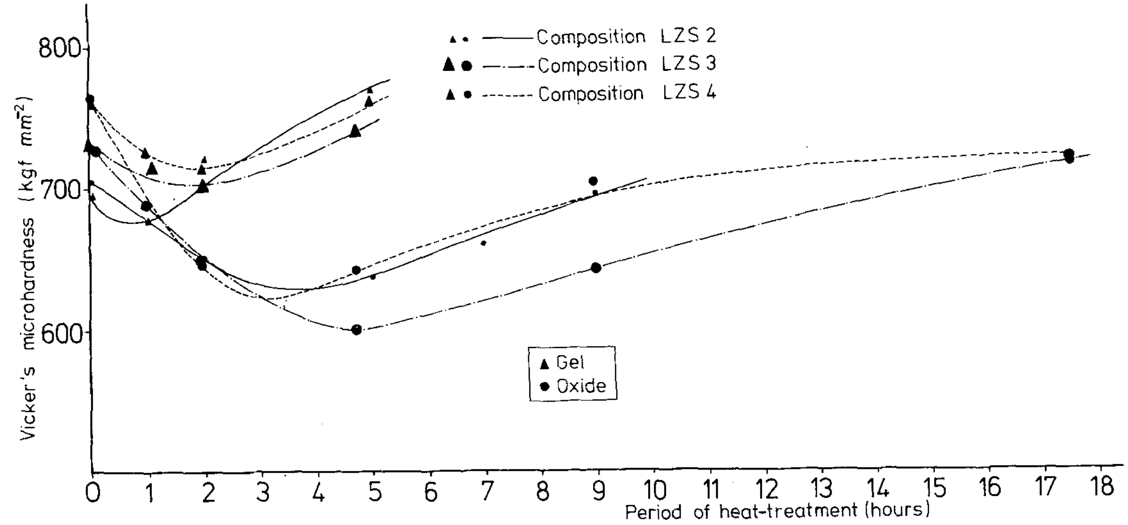

Figure 11 Relation between the Vicker's micro-hardness and the period of heat-treatment of compositions: LZS2, LZS3, LZS4.

(a) the Zr^{4+} ions when initially incorporated in the glass-structure, increase the strength [20], but on heat-treatment, the Zr^{4+} ions are removed from the glass structure and precipitate as ZrO_2;

(b) because of the low rate of nucleation, the mean free distance between the particles is larger;

(c) the coarsening which leads to large droplets and interconnected phases [21].

In the case of gel-glasses, the shape of the curves is different from those obtained with the ox-glasses. There is no sharp fall in micro-hardness, only a slight drop during the initial period of 1 h or 2 h, after which the micro-hardness increases very sharply and the shape of the curves is similar with all compositions.

This increased hardness of gel-glasses may be due to the following factors:

(a) during the initial period, the precipitation of ZrO_2 is less, and so, the Zr^{4+} ions remain in the glass structure, and increase the strength.

(b) coarsening does not occur;

(c) the higher rates of nucleation and crystallization give higher volume fractions of dispersed phase resulting in a small mean distance between the particles.

It may be stated in conclusion that the structure of gel-glass differs significantly from that of ox-glass, and as a consequence, the physico-chemical properties such as phase separation, nucleation and crystallization differ markedly. It does not seem possible, with the present experimental results, to clarify precisely the structural differences between the gel-glass and the ox-glass.

4. Conclusion

The following general conclusions can be drawn from the results obtained with different systems:

(i) The gelling technique which is normally used for the preparation of starting materials for solid-state reactions, can be advantageously utilized for the preparation of non-crystalline multicomponent inorganic oxides. The subsequent fusion of these "gels" produces glasses which are more homogeneous (in terms of phase separation) than those prepared from the mixture of oxides. It appears that the homogeneity and the structure of gels obtained during gel formation are inherited to a great extent by the glass.

(ii) It is also evident that the –OH groups which are not removed during the dehydration of the gels and are incorporated into the glass-structure have a great influence in increasing the nucleation and crystallization rates.

(iii) The formation of high temperature crystal form is more evident with the crystallization of gel-glasses.

(iv) Small additions of Al_2O_3 in place of SiO_2 to the binary SiO_2–La_2O_3 glass improve the homogeneity but decrease the micro-hardness and the rates of devitrification of the glasses.

(v) Small additions of ZrO_2 in place of SiO_2 to the binary SiO_2–La_2O_3 glass increase the micro-hardness but with increase of ZrO_2 content, devitrification occurs.

(vi) When the rate of nucleation is low, (as in the case of glasses from the mixture of oxides), the curve representing the relation between the micro-hardness and the periods of heat-treatment shows a distinct minimum, whereas this minimum is not obtained with the gel-glasses. With most of the gel-glasses, the micro-hardness rises sharply with the period of heat-treatment. The curve showing the relation between the micro-hardness and the volume fraction of the dispersed crystalline phase also gives a distinct minimum which could be explained on the basis of the fracture mechanism consisting of the processes of crack nucleation and of crack propagation around the dispersed crystalline particles.

Acknowledgement

The authors wish to thank the Délégation Générale à la Recherche Scientifique et Technique of Ministère du Développement Industriel et Scientifique for their financial suppor for this work.

References

1. R. ROY, *J. Amer. Ceram. Soc.* **39** (1956) 145.
2. W. C. RUTH and C. O. INGAMELLS, *Amer. Mineral* **50** (1965) 255.
3. G. M. BIGGAR and M. J. O'HARA, *Mineral. Mag.* **37** (1969) 198.
4. R. ROY, *J. Amer. Ceram. Soc.* **52** (1969) 344; **54** (1971) 639.
5. H. DISLICH, *Angew. Chemie. Intern. Edition* **10** (6) (1971) 363.
6. H. K. HENISCH, "Crystal growth in gels" (The Pennsylvania State University Press, 1970).
7. A. N. LAZAREV and M. G. VORONKOV, *Optics. Spectrosc.* 8 (1960) 325.
8. K. A. ANDRIANOV and A. A. ZHDANOV, *J. Polymer Sci.* **30** (1958) 513.
9. J. P. TRAVERSE and P. FLAMAND, "Symposium on Physico-chemical Techniques at High Temperature", Baden bei Wein, September 1973, p. 21.
10. J. P. TRAVERSE, M. FOEX and R. COLLONGUES, Congrès "Le Soleil au Service de l'Homme" Paris, 26 July 1973.

11. M. S. MAKLAD and N. J. KREIDL, IX International Congress on Glass, Versailles, France (1971).
12. L. AINSWORTH, *J. Soc. Glass. Tech.* 38 (1954) 479, 501, 536.
13. D. M. MARSH, *Proc. Roy. Soc. A* 282 (1964) 33.
14. G. M. BARTENEV, I.V. RAZUMOVSKAYA and D. S. SANDITOV, *J. Non-Cryst. Solids* 1 (1969) 388.
15. M. YAMANE and J. D. MACKENZIE, *ibid* 15 (1974) 153.
16. W. A. WEYL and E. MARBOE, "The Constitution of Glasses", Vol. I (Interscience, New York, 1962) p. 383.
17. A. PETZOLD, F. G. WIHSMANN and H. VON KAMPTZ, *Glastech. Ber.* 34 (1961) 56.
18. A. MAKISHIMA and J. D. MACKENZIE, *J. Non-Cryst. Solids* 12 (1973) 35.
19. W. A. WEYL and E. C. MARBOE, "The Constitution of Glasses", Vol. II, Part 1 (Interscience, New York, (1964) p. 511.
20. K. L. LOEWENSTEIN, *Phys. Chem. Glasses* 2 (1961) 69.
21. Y. UTSUMI and S. SAKKA, *Glass. Tech.* 11 (1970) 87.
22. A. CLEARFIELD and P. A. VAUGHAN, *Acta Cryst.* 9 (1956) 555.
23. J. M. FLETCHER and C. J. HARDY, *Chem. Ind.* January (1968) 48.
24. I. WARSHAW and R. ROY, "Progress in Science and Technology of the Rare Earths", Vol. 1 (Pergamon Press, New York, 1964) p. 215.
25. J. FELSCHE, *J. Less-Common Metals* 21 (1970) 1.
26. E. E. UNDERWOOD, A. R. COLCORD and R. C. WAUGH, "Ceramic microstructure", edited by R. M. Fulrath and J. A. Pask (John Wiley, New York, 1968) Ch. 1, p. 25.
27. S. P. MUKHERJEE and P. S. ROGERS, *Phys. Chem. Glasses* 8 (1967) 81.
28. M. J. BUERGER, *Amer. Mineral.* 33 (1948) 744.
29. A. G. VERDUCH, *J. Amer. Ceram. Soc.* 41 (1958) 427.
30. G. HETHERINGTON, K. H. JACK and J. C. KENNEDY, *Phys. Chem. Glasses* 5 (1969) 130.
31. F. E. WAGSTAFF, S. D. BROWN and I. B. CUTLER, *ibid* 5 (1964) 76.
32. D. M. DODD and D. B. FRASER, *Amer. Mineral.* 52 (1967) 140.
33. M. J. BUERGER in "Phase Transformation in Solids" edited by R. Smoluchowski *et al.* (John Wiley, New York 1951) Ch. 6, p. 196.
34. D. P. H. HASSELMAN and R. M. FULRATH. *J. Amer. Ceram. Soc.* 49 (1966) 68.
35. N. MIYATA and H. JINNO, *J. Mater. Sci.* 7 (1972) 973.
36. J. ZARZYCKI in "Recent Advances in Science and Technology of Materials" Vol. 2, edited by Adli Bishay (Plenum Press, New York, 1974) p. 193.
37. N. A. TOROPOV and I. A. BONDAR, *Izvest. Akad. Nauk SSSR Otdelenie Khim. Nauk* 5 (1961) 740.

Received 23 May and accepted 14 July 1975.